Journal of the European Ceramic Society 44 (2024) 116748

Contents lists available at ScienceDirect

Journal of the European Ceramic Society

journal homepage: www.elsevier.com/locate/jeurceramsoc

One-step additive manufacturing of melt-growth porous ceramics by laser directed energy deposition

Xuexin Yu [a], Dongjiang Wu [a], Xiao Feng [a], Cong Zhou [b], Bi Zhang [b], Huanyue Zhang [c], Qian Bai [a], Guangyi Ma [a], Fangyong Niu [a,*]

[a] State Key Laboratory of High-performance Precision Manufacturing, Dalian University of Technology, Dalian Liaoning 116024, PR China
[b] Department of Mechanical and Energy Engineering, Southern University of Science and Technology, Shenzhen, Guangdong 518055, PR China
[c] Instrumental Analysis Center, Dalian University of Technology, Dalian, Liaoning 116024, PR China

ARTICLE INFO

Keywords:
Porous ceramic
Laser directed energy deposition
Additive manufacturing

ABSTRACT

Porous ceramics, as a new type of lightweight ceramic materials, have attracted much attention in recent decades due to their low thermal conductivity and high surface area, which are crucial for applications in aerospace and biomedicine. In this work, we report a novel approach for the one-step additive manufacturing of melt-growth Al_2O_3-ZrO_2-SiCp porous ceramics using laser directed energy deposition (LDED). The fracture surfaces of as-fabricated specimens show obvious porous structures when SiCp content exceeds 50 wt%. The porosity and compressive strength of Al_2O_3-ZrO_2-70 wt% SiCp (AZS70) specimens can reach 48 ± 4 % and 95 ± 5 MPa, respectively. In addition, the compressive strength of AZS70 is found to increase by a factor of 2–3 compared to the case of oxide porous ceramics with similar porosity prepared by other additive manufacturing technologies. Our approach may provide a valid option for achieving porous ceramics with excellent mechanical properties.

1. Introduction

Porous ceramics, recognized as a promising lightweight and high-performance ceramic material, have been widely desirable for widespread applications in aerospace, environmental catalysis, and biomedicine owing to their outstanding low thermal conductivity, good chemical stability, and significant noise reduction capabilities [1–6]. On the one hand, porous ceramics with porosity similar to that of human bone can be used as scaffolds in bio-bone implants, which is conducive to the accelerated healing of skeletal injuries. On the other hand, the porous structures offer excellent adsorption capacity for automobile exhaust treatment, significantly reducing environmental damage. Combining the superior mechanical properties of Al_2O_3-ZrO_2 eutectic ceramics (including hardness, fracture toughness, and high-temperature stability) with the exceptional oxidation and corrosion resistance of SiCp, melt-growth Al_2O_3-ZrO_2-SiCp porous ceramics are expected to be widely used in complex service environments.

Conventional methods for fabricating porous ceramics, such as direct foaming [7], freeze casting [8], and gel casting [9], require preparing porous ceramic green bodies before sintering. Additionally, most of these methods are limited by equipment and fabrication principles, making it difficult to manufacture porous ceramics with arbitrary geometries. Recently, researchers have begun to pay attention to using additive manufacturing, such as stereolithography (SLA) [10] and direct ink writing (DIW) [11], for porous ceramics. Additive manufacturing not only enables the preparation of porous ceramics with complex shapes but also allows for the on-demand design of pore size and porosity to meet the requirements of practical applications. However, additive manufacturing currently in use still needs supplementary steps like sintering for final components. These steps could lead to deformation and cracking, potentially resulting in component failure.

LDED is an additive manufacturing technology that utilizes a laser beam to melt material and fabricate components layer by layer. Compared to conventional preparation methods, LDED does not require subsequent sintering, enabling the one-step fabrication of ceramic components. In recent years, LDED has been increasingly applied in the research of melt-growth ceramics [12–17]. In this work, we utilize LDED to fabricate Al_2O_3-ZrO_2-SiCp composite porous ceramics for the first time, which provided a valid option for achieving porous ceramics with excellent mechanical properties.

* Corresponding author.
E-mail address: niufangyong@dlut.edu.cn (F. Niu).

https://doi.org/10.1016/j.jeurceramsoc.2024.116748
Received 29 April 2024; Received in revised form 8 July 2024; Accepted 12 July 2024
Available online 14 July 2024

2. Material and methods

The main equipment of the LDED system is shown in Fig. 1. The experiment utilized spherical Al_2O_3 powder (Ya'an Bestry Performance Materials Corporation) and ZrO_2 powder (Beijing Sunspraying New Materials Co., Ltd.) with a purity of over 99 %, which were blended and mechanically agitated with the proportion of 63 mol.% Al_2O_3-37 mol.% ZrO_2 (eutectic proportion). Subsequently, SiCp powder was added to the Al_2O_3-ZrO_2 eutectic powder in proportions of 30 wt% (AZS30), 50 wt% (AZS50), and 70 wt% (AZS70), respectively. The blended powder was then dried at 120 ℃ for more than 4 hours to remove moisture. The optimized deposition parameters were as follows: laser power of 300 W, scanning speed of 400 mm/min, layer thickness of 0.4 mm, and beam diameter of 2 mm. In the LDED experiments, cylindrical specimens with dimensions ϕ5 mm × 16 mm were shaped on an Al_2O_3 substrate under the argon atmosphere. The field emission scanning electron microscope (JSM-7900) was used to characterize the fracture surfaces and microstructure of the specimens. The porosity of specimens with different SiCp ratios, three in a set, was observed using a three-dimensional X-ray microscope (ZEISS Xradia 610 Versa). Compression tests on the as-fabricated specimens with different SiCp ratios were performed using a universal mechanical testing machine (WDW-20E). The values of compressive strength were determined by the average of five tests. To calculate the elastic modulus of the ceramic materials from the compression tests, the stress-strain curves were analyzed. The initial linear portion of the stress-strain curve, representing the elastic deformation region, was identified, and linear regression analysis was performed on this region. The slope of the resulting linear fit corresponds to the elastic modulus (E) of the material.

3. Results and discussion

3.1. Macroscopic morphology and fracture surface

Fig. 2 presents the typical macroscopic morphology and fracture surface of the as-fabricated specimens with varying SiCp contents. The AZS ceramics appear grey-black, while the presence of white material on the surface is the Al_2O_3-ZrO_2 eutectic powder adhered during the solidification. The surface of AZS30 is dense and free of porosity, exhibiting a uniformly dense microstructure on the fracture surface. As the SiCp content increases, tiny pores appear on the surface of AZS50, and pores are also evident on the fracture surface. For AZS70, there is a substantial increase in the number of surface pores, and the fracture surface exhibits a loose and porous structure.

3.2. Pore characteristics

Fig. 3(a) shows the XRT image of the AZS porous ceramic specimen, where different colors represent distinct pores. With the increase in SiCp content, there is a significant increase in the porosity of the specimens, as shown in Fig. 3(b), rising from AZS30 at 0.2 ± 0.1 % to AZS70 at 48 ± 4 %. Statistical analysis using independent sample t-tests revealed significant differences between all pairs: AZS30 vs AZS50 (p-value = 0.0043), AZS30 vs AZS70 (p-value = 0.0031), and AZS50 vs AZS70 (p-value = 0.0065). Fig. 3(c) shows the distribution of the pores on the fracture surface, where most pores are unfused and surrounded by SiCp (Fig. 3(d)). SiCp is present as unmelted particles in the as-fabricated specimens [16]. With a higher proportion of SiCp, the quantity of Al_2O_3-ZrO_2 eutectic powder available for melting and forming the melt pool diminishes, leading to the deterioration of the flowability of the melt pool. Furthermore, the dense distribution of SiCp particles in the melt pool hinders the connectivity of the Al_2O_3-ZrO_2 melt. As a result, the melt fails to fill the gaps between SiCp before solidifying, resulting in the formation of unfused pores [17].

3.3. Compressive strength

Fig. 4(a) indicates the relationship between the compressive strength of specimens and the different SiCp content. As the SiCp content increases, the compressive strength decreases from 414 ± 22 MPa for AZS30 to 95 ± 5 MPa for AZS70, a decline of approximately 77 %. The statistical significance of the differences in compressive strength between the groups was confirmed with p-values well below the 0.05 threshold: AZS30 vs AZS50 ($p = 3.405e^{-12}$), AZS30 vs AZS70 ($p = 1.141e^{-12}$), and AZS50 vs AZS70 ($p = 2.002e^{-9}$). Similarly, the elastic modulus decreases significantly with increasing SiCp content, dropping from 23 ± 3 GPa for AZS30 to 4 ± 1 GPa for AZS70. The strength-porosity relations given by Ryskewitsch's empirical formula [17] are expressed as:

$$\sigma_c = \sigma_0 \exp(-nQ) \quad (1)$$

Where σ_c is the compressive strength, Q is the porosity of the specimen, n is a constant, and σ_0 is the compressive strength at Q=0. During the compression tests, the applied load causes stress concentration at the pores within the specimen, leading to specimen failure. Consequently,

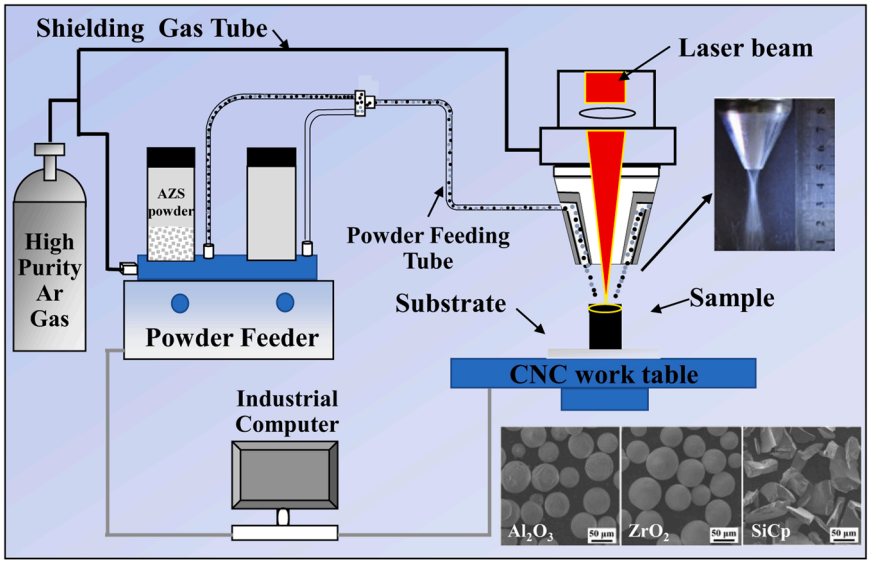

Fig. 1. LDED system.

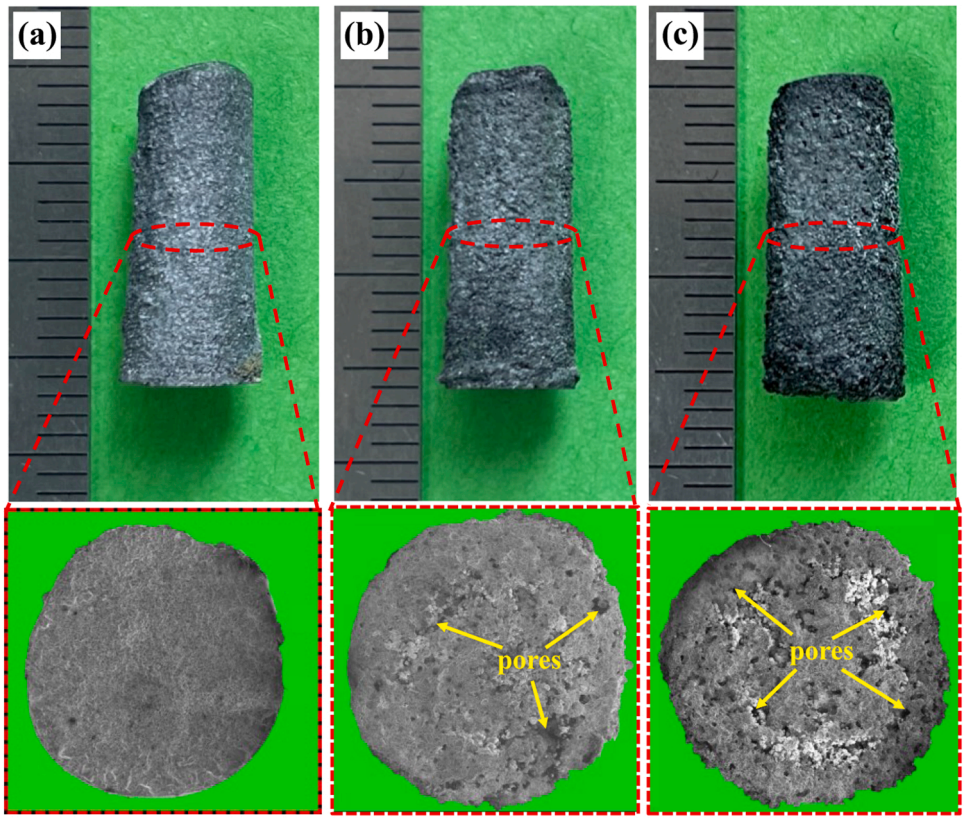

Fig. 2. Morphology and fracture surface of specimens with different SiCp contents: (a)AZS30; (b)AZS50; (c)AZS70.

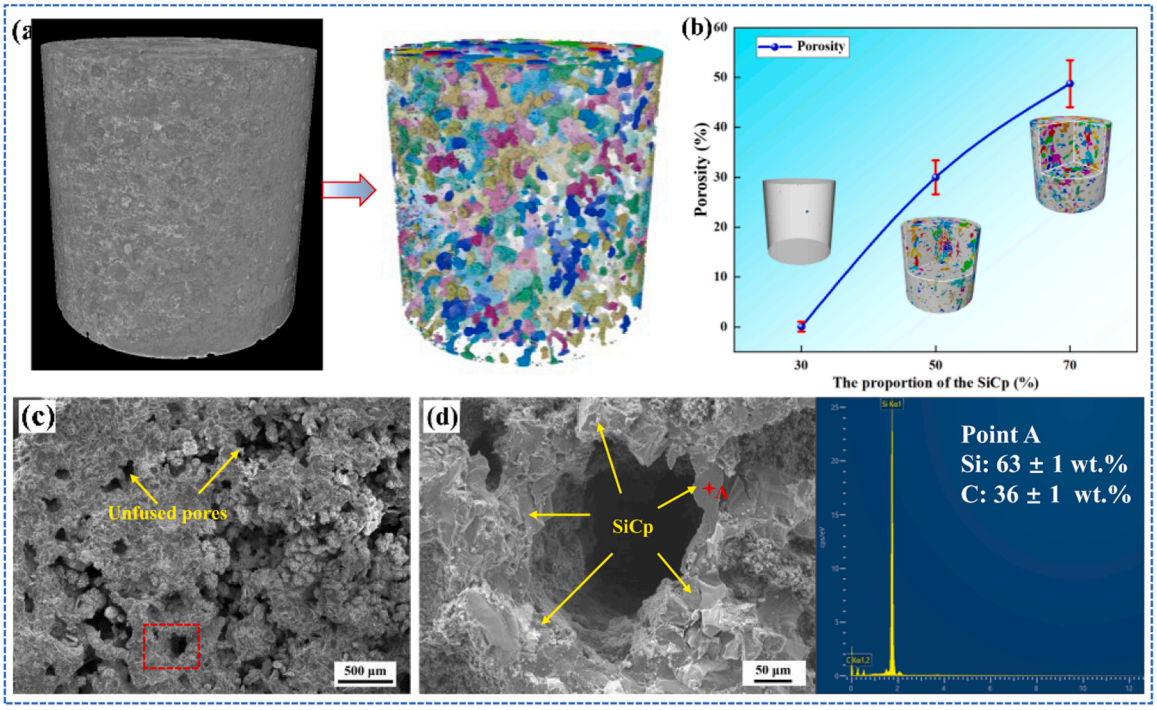

Fig. 3. Characteristics of pores: (a) XRT image; (b) Relationship between porosity and SiCp content; (c) Pores distribution on the fracture surface; (d) Unfused pores.

the compressive strength of the specimen significantly decreases as the porosity increases. The SEM image (Fig. 4(c)) shows the fracture surface of the as-fabricated specimen after compression testing. Many cleavage steps can be seen on the fracture surface, composed of SiCp (Fig. 4(d)). In this case, the dense distribution of SiCp results in a higher energy requirement for the as-fabricated specimen to fracture, which determines the fracture load and hence the strength. When compared with oxide porous ceramics prepared by other additive manufacturing

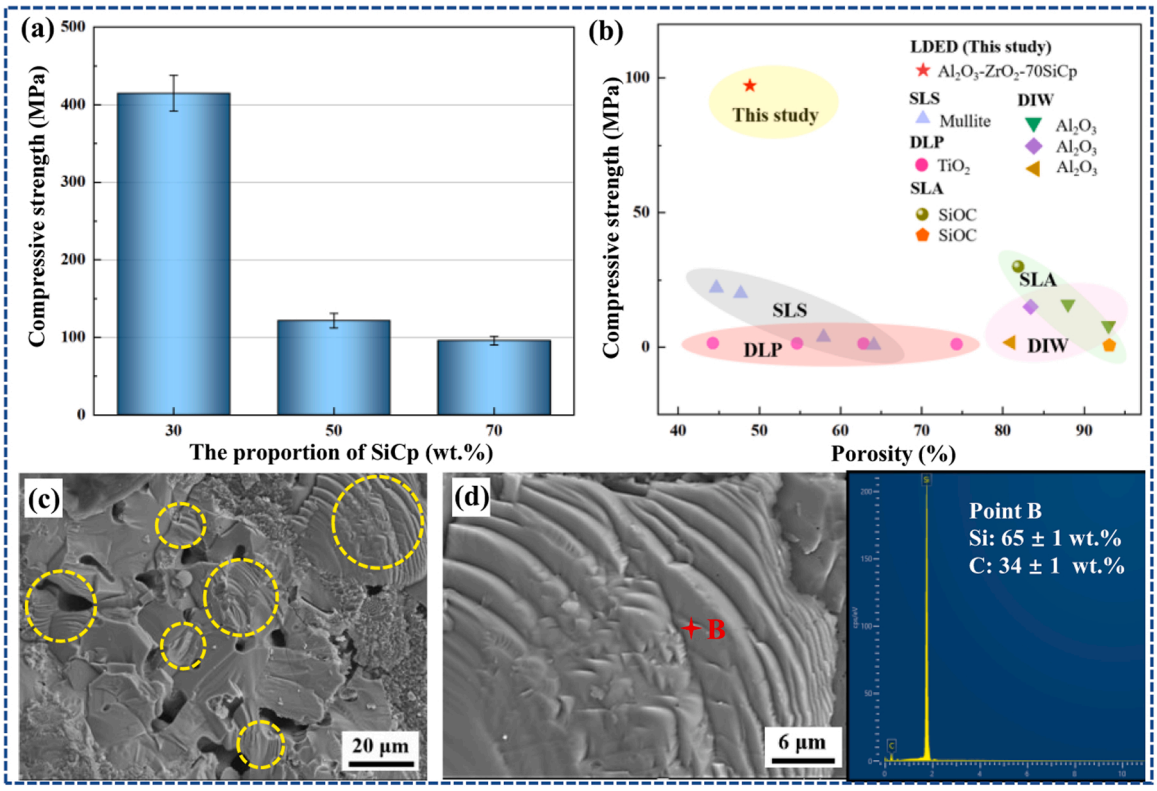

Fig. 4. Compressive strength of porous ceramics: (a) Relationship between compressive strength and SiCp content; (b) Comparison of the compressive strength of AZS70 with oxide ceramics prepared by other additive manufacturing techniques (Mullite—SLS [18], Al_2O_3—DIW [19–21], TiO_2—DLP [22], SiOC—SLA [23,24]); (c) Fracture surface of specimens after compression testing; (d) EDS analysis of cleavage step.

techniques (Fig. 4(b)) [18–25], it is notable that the compressive strength of AZS70 fabricated by LDED in this study is found to increase by a factor of 2–3 at similar porosity levels.

4. Conclusion

In summary, Al_2O_3-ZrO_2-SiCp composite porous ceramics were successfully prepared by LDED for the first time, introducing a novel method for porous ceramics fabrication. The pores in the as-fabricated specimens are primarily unfused pores formed when the melt fails to fill gaps during solidification. The porosity increases from 0.2 ± 0.1 % to 48 ± 4 %, and the compressive strength decreases from 414 ± 22 MPa to 95 ± 5 MPa, as the content of SiCp increases from 30 wt% to 70 wt%. Although the porosity of AZS70, prepared by LDED, is comparatively lower than that of oxide porous ceramics fabricated through other additive manufacturing techniques, the compressive strength of AZS70 is found to increase by a factor of 2–3 at equivalent porosity levels.

CRediT authorship contribution statement

Huanyue Zhang: Resources, Funding acquisition. **Bi Zhang:** Resources, Funding acquisition. **Cong Zhou:** Resources, Funding acquisition. **Fangyong Niu:** Validation, Resources, Project administration, Methodology, Investigation, Funding acquisition, Formal analysis, Data curation, Conceptualization. **Guangyi Ma:** Resources, Funding acquisition. **Qian Bai:** Resources, Funding acquisition. **Xiao Feng:** Writing – review & editing, Validation, Investigation. **Dongjiang Wu:** Methodology, Investigation, Funding acquisition, Formal analysis, Conceptualization. **Xuexin Yu:** Writing – review & editing, Writing – original draft, Visualization, Validation, Methodology, Investigation, Conceptualization.

Declaration of Competing Interest

The authors declare that they have no known competing financial interests or personal relationships that could have appeared to influence the work reported in this paper.

Acknowledgements

This work was funded by the National Natural Science Foundation of China (No. 52375312), Fundamental Research Funds for the Central Universities (No. DUT23YG230), National Key Research and Development Program of China (2023YFB4605900, 2022YFB3403401), Liaoning Province Science and Technology Plan Joint Program (2023JH2/101700299), Shenzhen Science and Technology Innovation Commission (JCYJ20210324115413036), Science Center for Gas Turbine Project (P2022-B-IV-012-001).

References

[1] J.F. Li, H. Lin, J.B. Li, Factors that influence the flexural strength of SiC-based porous ceramics used for hot gas filter support, J. Eur. Ceram. Soc. 31 (2011) 825–831, https://doi.org/10.1016/j.jeurceramsoc.2010.11.033.
[2] D.J. Wu, X.T. Cai, X. Qin, F. Yang, R.K. Kang, Z.G. Dong, G.Y. Ma, Y. Bao, F.Y. Niu, Laser ablation behavior and mechanism of C_f/C–SiC composites under different laser energy densities, Compos. Part B-Eng. 276 (2024) 111359, https://doi.org/10.1016/j.compositesb.2024.111359.
[3] G.L. Gary, A.J. Stevenson, Toward pore-free ceramics, Science 322 (2008) 381–383, https://doi.org/10.1126/science.1160903.
[4] Y.K. Kim, Y.J. Jin, J.H. Song, H.D. Kim, Engineering porosity in silicon carbide ceramics, J. Mater. Sci. 45 (2010) 2808–2815, https://doi.org/10.1007/s10853-010-4270-5.
[5] P. Colombo, G. Mera, R. Riedel, G.D. Sorarù, Polymer-derived ceramics: 40 years of research and innovation in advanced ceramics, J. Am. Ceram. Soc. 45 (2010) 1805–1837, https://doi.org/10.1111/j.1551-2916.2010.03876.x.
[6] Z.G. Hou, H.Y. Du, J.C. Liu, R.H. Hao, X. Dong, M.X. Liu, Fabrication and properties of mullite fiber matrix porous ceramics by a TBA-based gel-casting process, J. Eur.

Ceram. Soc. 33 (2013) 717–725, https://doi.org/10.1016/j.jeurceramsoc.2012.10.011.
[7] C.L. Xu, H.R. Liu, H.L. Yang, L. Yang, A green biocompatible fabrication of highly porous functional ceramics with high strength and controllable pore structures, J. Mater. Sci. Technol. 32 (2016) 729–732, https://doi.org/10.1016/j.jmst.2016.07.002.
[8] Z. Wu, L.C. Sun, J.J. Pan, J.Y. Wang, Fiber reinforced highly porous γ-$Y_2Si_2O_7$ ceramic fabricated by foam-gelcasting-freeze drying method, Scr. Mater. 146 (2018) 331–334, https://doi.org/10.1016/j.scriptamat.2017.12.017.
[9] F.Z. Zhang, T. Kato, M. Fuji, M. Takahashi, Gelcasting fabrication of porous ceramics using a continuous process, J. Eur. Ceram. Soc. 26 (2006) 667–671, https://doi.org/10.1016/j.jeurceramsoc.2005.07.021.
[10] J.X. Sun, J. Binner, J.M. Bai, 3D printing of zirconia via digital light processing: optimization of slurry and debinding process, J. Eur. Ceram. Soc. 40 (2020) 5837–5844, https://doi.org/10.1016/j.jeurceramsoc.2020.05.079.
[11] G.Y. Yang, R.H. Guan, H.Y. Zhen, K.T. Ou, J. Fang, D.S. Li, Q. Fu, Y.Y. Sun, Tunable size of hhierarchically porous alumina ceramics based on DIW 3D pprinting supramolecular Gel, ACS Appl. Mater. Interfaces 14 (2022) 10998–11005, https://doi.org/10.1021/acsami.1c24090.
[12] V.K. Balla, S. Bose, A. Bandyopadhyay, Processing of bulk alumina ceramics using laser engineered net shaping, Int. J. Appl. Ceram. Tec. 5 (2008) 234–242, https://doi.org/10.1111/j.1744-7402.2008.02202.x.
[13] Z.Q. Fan, Q.Y. Tan, C.W. Kang, H. Huang, Advances and challenges in direct additive manufacturing of dense ceramic oxides, Int. J. Extrem. Manuf. 6 (2024) 052004, https://doi.org/10.1088/2631-7990/ad5424.
[14] H. Jiang, H.J. Su, M.H. Yu, J.T. Yao, Q. Chen, Z.L. Shen, X. Li, D. Dong, M. Guo, Z. Zhang, Insights into the influence of powder particle shape on forming process and mechanical properties of Al_2O_3 ceramic fabricated by laser directed energy deposition, Addit. Manuf. 81 (2024) 103984, https://doi.org/10.1016/j.addma.2024.103984.
[15] X.X. Yu, D.J. Wu, W.M. Bi, X. Feng, Z.Y. Zhao, Y.B. Hao, G.Y. Ma, C. Zhou, F.Y. Niu, Direct additive manufacturing of Al_2O_3–TiCp functionally graded ceramics by laser-directed energy deposition, J. Am. Ceram. Soc. 107 (2024) 3522–3533, https://doi.org/10.1111/jace.19653.
[16] D.J. Wu, F. Lu, D.K. Zhao, G.Y. Ma, C.J. Li, J. Ding, F.Y. Niu, Effect of doping SiC particles on cracks and pores of Al_2O_3-ZrO_2 eutectic ceramics fabricated by directed laser deposition, J. Mater. Sci. 54 (2019) 9321–9330, https://doi.org/10.1007/s10853-019-03555-z.
[17] D.J. Wu, X.X. Yu, Z.Y. Zhao, G.Y. Ma, C. Zhou, B. Zhang, G.H. Ren, F.Y. Niu, One-step additive manufacturing of TiCp reinforced Al_2O_3-ZrO_2 eutectic ceramics composites by laser directed energy deposition, Ceram. Int. 49 (2023) 12758–12771, https://doi.org/10.1016/j.ceramint.2022.12.141.
[18] A.N. Chen, L. Lu, L.J. Cheng, R.Z. Liu, S. Chen, Y. Chen, S.F. Wen, C.H. Li, Y.S. Shi, TEM analysis and mechanical strengthening mechanism of MnO_2 sintering aid in selective laser sintered porous mullites, J. Alloy Compd. 809 (2019) 151809, https://doi.org/10.1016/j.jallcom.2019.151809.
[19] C. Minas, D. Carnelli, E. Tervoort, A.R. Studart, 3D Printing of emulsions and foams into hierarchical porous ceramics, Adv. Mater. 28 (2016) 9993–9999, https://doi.org/10.1002/adma.201603390.
[20] J.T. Muth, P.G. Dixon, L. Woish, J.A. Lewis, Architected cellular ceramics with tailored stiffness via direct foam writing, P. Natl. Acad. Sci. USA 114 (2017) 1832–1837, https://doi.org/10.1073/pnas.1616769114.
[21] M. Schumacher, U. Deisinger, R. Detsch, G. Ziegler, Indirect rapid prototyping of biphasic calcium phosphate scaffolds as bone substitutes: influence of phase composition, macroporosity and pore geometry on mechanical properties, J. Mater. Sci. 21 (2010) 3119–3127, https://doi.org/10.1007/s10856-010-4166-6.
[22] J. Guo, Y. Zeng, P.R. Li, J.M. Chen, Fine lattice structural titanium dioxide ceramic produced by DLP 3D printing, Ceram. Int. 45 (2019) 23007–23012, https://doi.org/10.1016/j.ceramint.2019.07.346.
[23] Z.C. Eckel, C.Y. Zhou, J.H. Martin, A.J. Jacobsen, W.B. Carter, T.A. Schaedler, Additive manufacturing of polymer-derived ceramics, Science 351 (2016) 58–62, https://doi.org/10.1126/science.aad2688.
[24] E. Zanchetta, M. Cattaldo, G. Franchin, M. Schwentenwein, J. Homa, G. Brusatin, P. Colombo, Stereolithography of SiOC ceramic microcomponents, Adv. Mater. 28 (2015) 370–376, https://doi.org/10.1002/adma.201503470.
[25] F. Zhang, Z.A. Li, M.J. Xu, S.Y. Wang, J.Q. Yang, A review of 3D printed porous ceramics, J. Eur. Ceram. Soc. 42 (2022) 3351–3373, https://doi.org/10.1016/j.jeurceramsoc.2022.02.039.